Bacterial genotoxin triggers FEN1-dependent RhoA activation, cytoskeleton remodeling and cell survival

Lina Guerra[1,*], Riccardo Guidi[1,*], Ilse Slot[1], Simone Callegari[1], Ramakrishna Sompallae[1], Carol L. Pickett[2], Stefan Åström[3], Frederik Eisele[4], Dieter Wolf[4], Camilla Sjögren[1], Maria G. Masucci[1] and Teresa Frisan[1,‡]

[1]Department of Cell and Molecular Biology, Karolinska Institutet, Box 285, S-171 77 Stockholm, Sweden
[2]Department of Microbiology and Immunology, Chandler Medical Center, University of Kentucky, Lexington, KY 40536-0298, USA
[3]Department of Developmental Biology, Wenner-Grens Institutet, Stockholm University, 106 91 Stockholm, Sweden
[4]Institute of Biochemistry, University of Stuttgart, 70569 Stuttgart, Germany

*These authors contributed equally to this work
‡Author for correspondence (Teresa.Frisan@ki.se)

Accepted 15 April 2011
Journal of Cell Science 124, 2735-2742
© 2011. Published by The Company of Biologists Ltd
doi:10.1242/jcs.085845

Summary

The DNA damage response triggered by bacterial cytolethal distending toxins (CDTs) is associated with activation of the actin-regulating protein RhoA and phosphorylation of the downstream-regulated mitogen-activated protein kinase (MAPK) p38, which promotes the survival of intoxicated (i.e. cells exposed to a bacterial toxin) cells. To identify the effectors of this CDT-induced survival response, we screened a library of 4492 *Saccharomyces cerevisiae* mutants that carry deletions in nonessential genes for reduced growth following inducible expression of CdtB. We identified 78 genes whose deletion confers hypersensitivity to toxin. Bioinformatics analysis revealed that DNA repair and endocytosis were the two most overrepresented signaling pathways. Among the human orthologs present in our data set, FEN1 and TSG101 regulate DNA repair and endocytosis, respectively, and also share common interacting partners with RhoA. We further demonstrate that FEN1, but not TSG101, regulates cell survival, MAPK p38 phosphorylation, RhoA activation and actin cytoskeleton reorganization in response to DNA damage. Our data reveal a previously unrecognized crosstalk between DNA damage and cytoskeleton dynamics in the regulation of cell survival, and might provide new insights on the role of chronic bacteria infection in carcinogenesis.

Key words: Cytolethal distending toxin, DNA damage, FEN1, Cell survival, TSG101, RhoA, Actin cytoskeleton

Introduction

Cytolethal distending toxins (CDTs) are produced by a variety of Gram-negative bacteria, such as *Escherichia coli*, *Aggregatibacter actinomycetemcomitans*, *Haemophilus ducreyi*, *Shigella dysenteriae*, *Campylobacter* sp. and *Helicobacter* sp., and *Salmonella enterica* (reviewed in Smith and Bayles, 2006). CDT activity requires the function of three genes (*cdtA*, *cdtB* and *cdtC*) and the active holotoxin is a tripartite complex (Lara-Tejero and Galan, 2001; Scott and Kaper, 1994), formed by the three subunits CdtA, CdtB and CdtC. The CdtB component is the active subunit, that shares structural and functional homology with the mammalian deoxyribonuclease I (DNase I) (Elwell et al., 2001; Lara-Tejero and Galan, 2000; Nesic et al., 2004). The CdtA and CdtC subunits are ricin-like lectin domains (Nesic et al., 2004), important for the cellular internalization of the toxin (Lee et al., 2003; McSweeney and Dreyfus, 2004; McSweeney and Dreyfus, 2005).

The capacity of CDT to induce DNA double-strand breaks (DSBs) was confirmed in intoxicated (i.e. cells exposed to a bacterial toxin) mammalian cells by pulsed-field gel electrophoresis (PFGE) (Frisan et al., 2003). Similar results were obtained by Hassane and co-workers who observed DSBs in *Saccharomyces cerevisiae* cells transfected with the active CdtB subunit (Hassane et al., 2001). In both cases, mutations within the DNase-conserved motives prevented induction of DNA damage.

The cellular effects of CDTs are similar to those induced by exposure to ionizing radiation (γ-irradiation), a well-characterized DNA-damaging agent. Both CDT and ionizing radiation stimulate the phosphorylation of histone H2AX and the relocalization of the DNA repair protein complex Mre11–Rad50–Nbs1 (MRN) (Hassane et al., 2003; Li et al., 2002). Both agents also activate cell cycle checkpoints in a cell-type-dependent manner (human primary fibroblasts are arrested in G1 and G2 phases, whereas HeLa cells are arrested in G2) (Cortes-Bratti et al., 2001; Hassane et al., 2003).

In adherent cells, γ-irradiation or CDT intoxication are associated with the formation of actin stress fibers (Cortes-Bratti et al., 1999; Gelfanova et al., 1999). This effect is regulated by the activation of the small GTPase RhoA, and promotes cell survival in intoxicated cells (Frisan et al., 2003). Activation of RhoA and actin stress fiber formation in response to CDT is dependent on the RhoA-specific guanine nucleotide exchange factor (GEF) Net1 (Guerra et al., 2008a).

The DNA-damage-dependent Net1–RhoA signaling diverges into two different effector cascades: one dependent on the RhoA kinases ROCKI and ROCKII that controls the formation of actin stress fibers, and one regulated by the mitogen-activated protein kinase (MAPK) p38 and its downstream target MAPK-activated protein kinase 2 (MAPKAPK2) that promotes cell survival (Guerra et al., 2008a).

The survival of cells with damaged DNA may promote genomic instability and favor tumor initiation and/or progression (reviewed in Kastan and Bartek, 2004; Shiloh, 2003). Characterization of the survival signals in response to CDTs is, therefore, relevant to understand how bacterial infections contribute to carcinogenesis. To identify new CDT-induced survival signals, we have screened a yeast deletion library in cells that express the active CdtB subunit under the control of a galactose-inducible promoter. This

screen identified 78 deletion mutants with a reduced growth rate following the inducible expression of CdtB. Bioinformatics analysis revealed that 12 human orthologs of these genes interacts with the RhoA signaling pathway. Functional studies in mammalian cells showed that flap structure-specific endonuclease 1) *FEN1* (yeast ortholog *RAD27*) promotes RhoA activation, MAPK p38 phosphorylation and, ultimately, cell survival in response to CDTs.

Results

Screening of the *S. cerevisiae* deletion library

CDT-induced DNA damage is accompanied by activation of the small GTPase RhoA, actin cytoskeleton rearrangements and phosphorylation of the downstream-regulated MAPK p38, which leads to delayed cell death (Guerra et al., 2008a). To identify the effectors of this survival response, we expressed the active subunit CdtB of the *Campylobacter jejuni* CDT under the control of a galactose-inducible promoter in the *S. cerevisiae* strain BY4743. Induction of CdtB expression by addition of galactose to the culture medium (CdtB ON) induced G2 arrest (supplementary material Fig. S1A) and inhibited cell growth (supplementary material Fig. S1B) in cells transformed with the pDCH-CdtB plasmid, whereas no effect was observed in cell grown in presence of glucose (CdtB OFF) or in cells transformed with the vector control.

Having confirmed the capacity of CdtB to induce cell cycle arrest, which was demonstrated to be dependent on the DNase activity of the toxin (Hassane et al., 2001), we performed a genome-wide screen using the EUROpean *Saccharomyces cerevisiae* ARchive for Functional analysis (EUROSCARF) library, derived from the BY4743 strain (Cherry et al., 1998), where nonessential genes are individually deleted. Deletion strains that showed growth aberrations, such as respiration deficiency (petite strains), were excluded. Of the 4793 deletion mutants 4085 were recovered on YPGluc plates and were successfully transformed with the CdtB-expressing pDCH–CdtB plasmid using the high-throughput yeast transformation method (Schafer and Wolf, 2005). To identify mutants with increased sensitivity to CdtB, serial dilutions of the transfected yeast were performed on plates containing selective medium supplemented with either glucose (CdtB OFF) or galactose/raffinose (CdtB ON) to regulate CdtB expression.

As expected, the growth of wild type (wt) cells was reduced in galactose/raffinose, compared with those grown in glucose. However, several deletion mutants showed a more pronounced inhibition of growth upon induction of CdtB expression (Fig. 1A, left panel). We defined as CdtB hypersensitive, deletion strains that did not grow after the third dilution step upon induction of CdtB expression. A total of 121 hypersensitive transformants were identified in three independent screens (Fig. 1A, right panel). To ensure that the reduced growth was due to the expression of CdtB rather than an intrinsic property of the deletion, each of the 121 mutants was transformed with a control empty plasmid, and a serial dilution screen in the presence or absence of galactose/raffinose was performed (data not shown). This analysis restricted the number of CdtB-hypersensitive mutants to 78 (Table 1). PCR analysis, performed for 30 of the 78 mutants, demonstrated that all the clones tested carried the correct deletion and validated the quality of the library used in this study (supplementary material Tables S1 and S2).

The identity of the yeast genes whose deletion confers hypersensitivity to CdtB is summarized in Table 1. On the basis of the annotated function in the *Saccharomyces* Genome Database (http://yeastgenome.org), we classified these genes into twelve

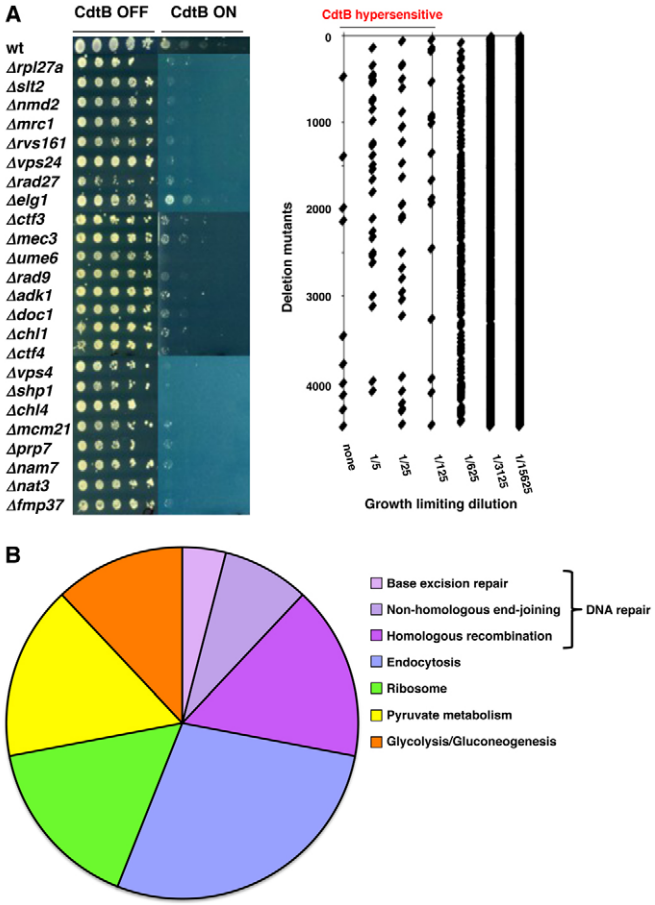

Fig. 1. Screening of the EUROSCARF deletion library. (**A**) Replica plating of fivefold serial dilutions of the wild-type (wt) cells or deletion mutants, transformed with the pDCH-CdtB plasmid, were incubated on plates that contained selective medium supplemented with 2% glucose (CdtB OFF) or 2% galactose/raffinose (CdtB ON) at 30°C for 48 hours. The left panel shows a selection of the tranformants. The right panel summarizes the growth pattern of all 4085 transformants. Each diamond represents the last dilution at which cell growth was detected. Strains that failed to grow after the third dilution (1/125) were scored as CdtB hypersensitive. (**B**) Pathway enrichment analysis was performed as described in Materials and Methods using as data set the 59 human orthologs of the 78 yeast genes found in the EUROSCARF library.

groups. Five genes could not be grouped because they encode proteins with unknown function. As expected, the majority of the genes conferring hypersensitivity to CdtB encode for proteins involved in the regulation of the DNA damage checkpoint responses, genome integrity and DNA repair (39%, groups 1-4). The next largest functional group comprised genes encoding for effectors involved in the control of vesicular transport and endocytosis (13%, group 5).

Using the Inparanoid database (O'Brien et al., 2005) and BLAST sequence alignment we identified 59 human orthologs of the 78 yeast genes found in the EUROSCARF library screening (Table 1). In agreement with the functional classification in the yeast data set, pathway enrichment analysis performed on the human orthologs demonstrated that DNA repair and endocytosis were the two most over-represented signaling pathways, followed by glucose metabolism and ribosome biogenesis (Fig. 1B and supplementary material Fig. S2).

Table 1. Genes identified in the EUROSCARF screen

Group	Function	Number of genes	Yeast genes	Human orthologs
1	Replication recombination repair	13	*DCC1; DDC1; DIA2; ELG1; MMS4; MUS81; RAD27; RAD50; RAD51; RAD57; SAE2; SHU1; SRS2*	*DSCC1, DIAPH3, MUS81, FEN1, RAD50, RAD51, XRCC3, UBA2, UBE2B*
2	Checkpoint	5	*CHK1; MEC3; MRC1; RAD9; TOF1*	*CHEK1, PIP3-E, MRC1L.1, RAD9A*
3	Chromatin silencing telomeres	8	*CST6; ESC1; NAM7; NAT3; NMD2; NPT1; UPF3;* YPL205C	*CST6, UPF1, NAT5, UPF2, SLC17A1, UPF3A*
4	Mitotic chromosome transmission	5	*CHL1; CHL4; CTF4; MCM21; MCM22*	*DDX11, CENPN, REPS2, NFIC*
5	Vacuolar/Golgi/ endocytosis	10	*DRS2; PEP7; PEP12; PMR1; SNF7; VPS3; VPS4; VPS8; VPS21; VPS23; VPS24*	*ATP8A2, LAP3, STX12, ATP2C1, CHMP4B, VPS4B, VPS8, RAB5A, TSG101, VPS24*
6	Mitochondrial	8	*ADK1; ALT1; FMP37; HFA1; MRPL10; OAR1; PDB1; SOD2*	*AK2, GPT, MRPL10, PDHB, SOD2*
7	Cytokinesis, spindle, cytoskeleton rearrangements	6	*CTF3; NIP100; PTC1; RVS161; SLT2; SRV2*	*PTCH2, BIN3, MAPK7, CAP1*
8	Translation/Ribosomal	6	*KAP123; RPL27A; RPL36A; RPS0B; RPS17A; ZUO1*	*IPO4, RPL27A, RPL36AL, LOC387867, RPS17, DNAJC2*
9	Transcription/ RNA metabolism	3	*BUR2; CKA2; NPL3*	*CST4, CSNK2A1, TAF15,*
10	Ubiquitin proteasome system	2	*DOC1; SHP1*	*TBX6, NSFL1C*
12	Others	6	*LAT1; LIP5; MKC7; RTS1; TPD3; TPS1*	*DLAT, LIAS, PPP2R5C, PPP2R1A TPSAB1/TPSB2*
13	Unknown	5	YBR099C; YDR109C; YEL045C; YMR252C; YOR376W	
			78 genes	59 genes

Identification of candidate proteins regulating the RhoA-dependent survival signals

The aim of the genome-wide screen was to characterize new genes that regulate cell survival through RhoA activation in response to CDT-induced DNA damage in mammalian cells. To identify possible candidates, a RhoA protein–protein interaction network was generated using the Protein Interaction Network Analysis (PINA) (Wu et al., 2009). We next assessed whether any of the genes present in our data set encoded for proteins that share common interacting partners with RhoA. As shown in Fig. 2, the products of 12 human orthologs directly bind with RhoA-interacting proteins (Fig. 2). Three of these proteins belong to the two most over-represented pathways identified in Fig. 1B: FEN1 (DNA repair), TSG101 and RAB5A (endocytosis).

On the basis of this analysis, we selected two proteins, FEN1 and TSG101, one from each of the enriched signaling pathways, to assess whether these effectors regulate cell survival, RhoA activation and actin cytoskeleton remodeling in response to DNA damage in higher eukaryotic cells.

FEN1 prolongs cell survival in response to DNA damage

Expression of the endogenous TSG101 and FEN1 proteins was downregulated through RNA interference (RNAi) by transfection of specific small interfering RNAs (siRNAs) in HeLa cells 48 hours prior to toxin treatment or γ-irradiation. As negative control we included a scramble siRNA (scRNA) and siRNA that specifically targets *CSNK2B*, which was not identified in the yeast screen as a relevant gene to promote cell survival in response to DNA damage. Two independent siRNAs were used for each protein. Transfection with the two specific siRNAs induced ~80–90% reduction in the levels of expression of TSG101 and FEN1 (Fig. 3A). Knockdown of *TSG101*, *FEN1* or *CSNK2B* did not prevent CDT-induced cell cycle arrest (data not shown).

The first set of experiments aimed to investigate the role of TSG101 and FEN1 in inhibition of cell death upon treatment with CDT. Forty-eight hours after siRNA transfection, cells were left untreated or exposed to CDT. The number of cells undergoing cell death was assessed 48 hours after treatment through detection of the activated form of the pro-apoptotic protein Bax by using the conformation-dependent antibody 6A7 in immunofluorescence assays, and through assessment of the number of cells with nuclear fragmentation – a late marker of death (Fig. 3). CDT-intoxication-induced Bax activation in ~20% of the untransfected cells (data not shown) or in cells transfected with the control siRNA (scRNA) (Fig. 3C, left panel). A similar ratio of cell death was observed when expression of TSG101 or CSNK2B was downregulated by RNA interference (Fig. 3C, right panel). By contrast, knockdown of FEN1 resulted in a significant increase of Bax-positive cells upon toxin treatment, corresponding to an approximately fourfold

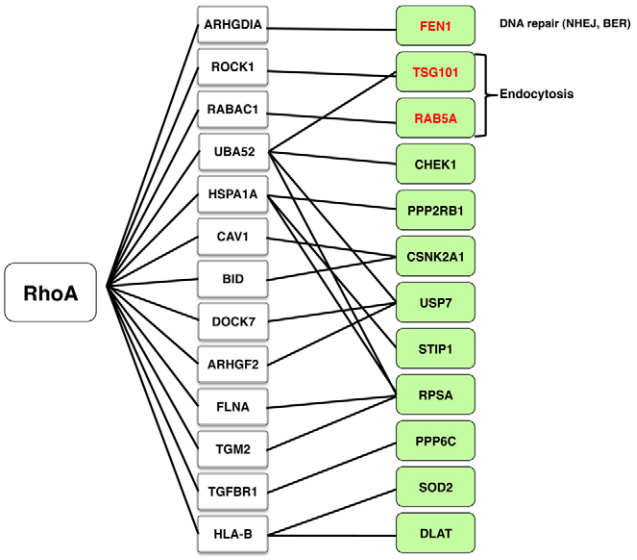

Fig. 2. RhoA protein–protein interaction network. The RhoA protein–protein interaction network was generated as described in Materials and Methods. The figure shows only interacting partners that are shared between RhoA and the products of the human orthologs present in our data set (green boxes). Proteins that belong to the two most-enriched pathways according to the analysis presented in Fig. 1B, are labelled in red.

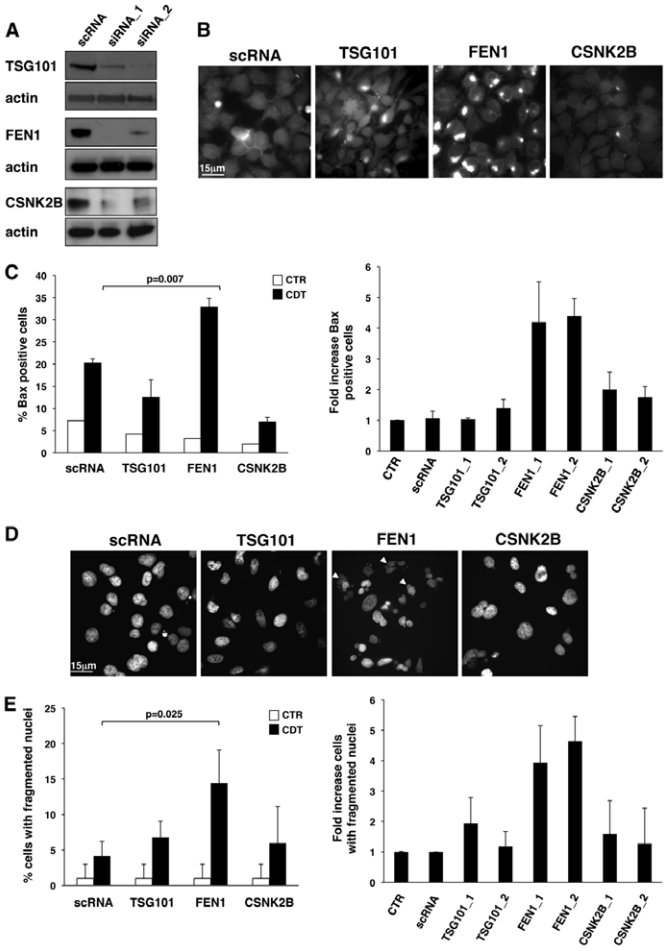

Fig. 3. FEN1 knockdown increases the rate of cell death upon induction of DNA damage. (**A**) HeLa cells were transfected with non-silencing siRNA (scRNA) or two specific siRNAs (indicated as _1 and _2) targeting *TSG101*, *FEN1* or *CSNK2B*. The individual siRNAs have been labeled as TSG101_1 and TSG101_2; FEN1_1 and FEN1-2; CSNK2B_1 and CSNK2B_2. Expression levels of the endogenous proteins were analyzed by western blotting 48 hours after transfection. Actin expression was assayed as loading control. (**B**) Cells transfected with non-silencing siRNA (scRNA), TSG101_1, FEN1_1, or CSNK2B_1 specific siRNA were left untreated (images not shown), or were exposed to CDT (2 μg/ml) for 48 hours. Apoptosis was assessed by immunofluorescence, using the conformation-dependent anti-Bax 6A7 antibody (magnification 63×). (**C**) Quantification of Bax-positive cells as percentage of Bax-positive cells (left panel) and as fold increase of Bax-positive cells (right panel). Fold increase is the ratio between the number of Bax-positive cells in intoxicated cells transfected with each specific siRNA and the number of Bax positive cells in intoxicated untransfected cells. Mean ± s.d. of three independent experiments. (**D**) HeLa cells transfected with non-silencing siRNA (scRNA), TSG101_1, FEN1_1, or CSNK2B_1 specific siRNA were left untreated (picture not shown) or exposed to CDT (2 μg/ml) for 48 hours. Nuclei were counterstained with Hoechst 33258 dye. (**E**) Quantification of cell death is shown as percentage of cells with fragmented nuclei (left panel) and as fold increase of cells with fragmented nuclei (right panel). Fold increase is the ratio between the number of cells with fragmented nuclei in intoxicated cells transfected with a specific siRNA versus the number of cells with fragmented nuclei in intoxicated untransfected cells. Mean ± s.d. of three independent experiments. For each experiment 100 cells were counted.

increase compared with the intoxicated untransfected cells (Fig. 3B,C). Similar data were obtained by monitoring the number of cells with fragmented nuclei. Intoxication-induced chromatin fragmentation in ~5% of intoxicated untransfected cells (data not shown) and in ~5% cells transfected with the control siRNA (scRNA) (Fig. 3D,E). The percentage of dying cells was not significantly increased upon downregulation of the endogenous levels of TSG101 and CSNK2B by siRNA. By contrast, 15–20% of intoxicated cells showed chromatin fragmentation upon FEN1 knockdown (Fig. 3E, left panel), corresponding to a three- to fourfold increase compared with intoxicated untransfected cells (Fig. 3E, right panel).

The late occurrence of CDT-induced cell death observed upon *FEN1* knockdown was similar to that observed in cells that express the dominant-negative form of RhoA (RhoAN19) and in cells where the expression of the RhoA-specific GEF Net1 was knocked down by siRNA (Frisan et al., 2003; Guerra et al., 2008a).

Induction of DNA DSBs stimulates the activation of the MAPK p38 in a RhoA-dependent manner; and this is required to delay cell death in response to toxin treatment or γ-irradiation (Guerra et al., 2008a). Since FEN1 appears to be required to promote cell survival, we tested whether it is also important for the activation of MAPK p38. A four- to fivefold increase in MAPK p38 activity was observed 4 hours after γ-irradiation in control HeLa cells or cells transfected with non-silencing siRNA, as assessed by western blot analysis using an antibody specifically recognizing phosphorylated MAPK p38 (Fig. 4). Similar levels of MAPK p38 phosphorylation were detected in irradiated HeLa cells, where expression of the endogenous levels of TSG101 or CSNK2B where knocked down with specific siRNA. Importantly, downregulation of FEN1 expression significantly decreased activation of MAPK p38 (Fig. 4).

RhoA activation and actin remodeling

We then assessed whether TSG101 and FEN1 are involved in the activation of RhoA and reorganization of the actin cytoskeleton in intoxicated or irradiated cells. As expected, intoxication or γ-irradiation induced an approximately threefold increase of RhoA activation in control cells or cells transfected with non-silencing siRNA 4h after treatment (Fig. 5A). Similar levels of GTP-bound RhoA were observed upon downregulation of the endogenous levels of TSG101, whereas knockdown of FEN1 completely prevented activation of this protein (Fig. 5A).

We also investigated whether FEN1-dependent inhibition of RhoA correlated with the reduction of stress fiber formation upon induction of DNA damage. Intoxication or γ-irradiation induced actin stress fibers in 50% of control cells or cells transfected with non-silencing siRNA 48 hours after treatment (Fig. 5B,C). Knockdown of the endogenous levels of TSG101 using siRNA did not significantly change stress fiber formation in treated cells. By contrast, FEN1 knockdown strongly reduced the number of cells carrying stress fibers upon exposure to CDT or γ-irradiation (Fig. 5B,C).

As a complementary evaluation of the level of actin polymerization upon induction of DNA damage, we have assessed the mean fluorescence intensity of phalloidin staining per cell area, measured using the *ImageJ* software (Fig. 5C, right panel). Intoxication or γ-irradiation induced a small increase of the mean fluorescence intensity in control cells, or in cells transfected with non-silencing siRNA or with the TSG101-specific siRNA compared with control untreated cells. By contrast, we observed a 50% reduction of the mean fluorescence intensity upon induction of DNA damage in cells whose levels of endogenous FEN1 were knocked down by siRNA. This effect was similar to that observed in cells expressing the dominant-negative form of RhoA

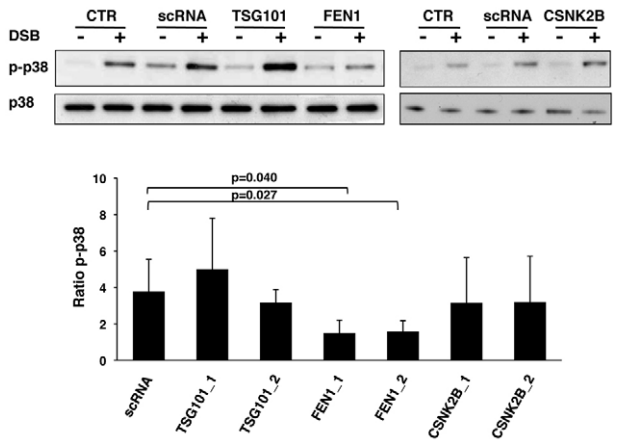

Fig. 4. FEN1-knockdown prevents phosphorylation of MAPK p38. Untransfected HeLa cells or cells transfected with non-silencing siRNA (scRNA), TSG101_1, FEN_1 or CSNK2B_1 specific siRNA were left untreated (–DSB), or exposed to ionizing radiation (20Gy, +DSB), and further incubated for 4 hours in complete medium. Samples were analyzed by western blot, using specific antibodies against phosphorylated MAPK p38 (p-p38) and MAPK p38 (p38) antibody. The bar graph represents the quantification of MAPK p38 activation (mean ± s.d. of three independent experiments). Data are the ratio between the optical density of the p-p38-specific band in irradiated cells and the optical density of the p-p38-specific band in untreated cells.

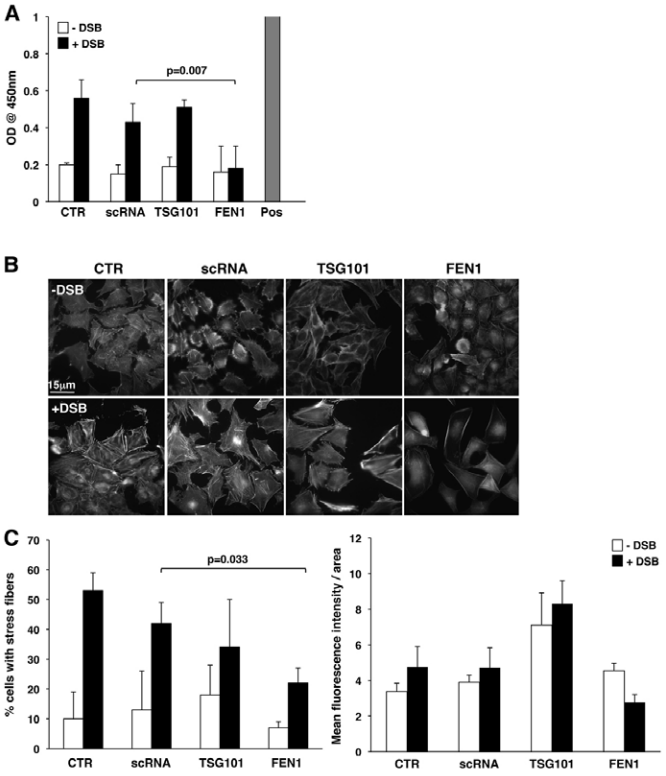

Fig. 5. RhoA activation and actin stress fiber formation upon knockdown of *FEN1* and *TSG101*. (**A**) Untransfected HeLa cells or cells transfected with non-silencing siRNA (scRNA), TSG101_1, or FEN1_1 specific siRNA were left untreated (–DSB) or exposed to CDT (2 µg/ml; +DSB) and were then further incubated for 4 hours. Activation of RhoA was assessed by using the RhoA-specific G-LISA™ kit (mean ± s.d. of three independent experiments). Pos, internal positive control of the RhoA-specific G-LISA™ assay. (**B**) Untransfected HeLa cells or cells transfected with non-silencing siRNA (scRNA), TSG101_1 or FEN1_1 specific siRNA were left untreated (–DSB) or exposed to CDT (2 µg/ml) for 48 hours (+DSB). The actin cytoskeleton was visualized by TRITC-phalloidin staining (magnification 63×). (**C**) Quantification of cells carrying stress fibers. The left panel shows the percentage of positive cells. Cells exhibiting more than five stress fibers were scored as positive. The right panel shows the ratio between the mean fluorescence intensity of the phalloidin staining and the cell area, quantified using the ImageJ software, as described in Materials and Methods. Mean ± s.e.m. of three independent experiments; 100 cells were counted for each experiment.

(RhoAN19) and in cells where the expression of the RhoA-specific GEF Net1 was knocked down by siRNA (Frisan et al., 2003; Guerra et al., 2008a).

In conclusion, our study demonstrates that FEN1 is a new effector in the RhoA-dependent signaling pathway that is activated in response to genotoxic stress (Fig. 6).

Discussion

The exact mechanism by which bacteria contribute to carcinogenesis is still poorly characterized. Several Gram-negative pathogenic bacteria have been shown to produce CDTs that induce DNA damage in infected cells. Since incorrect repair of DNA damage may lead to genomic instability and tumour development, it is conceivable that chronic infection with CDT-producing bacteria can be a risk factor for cancer development. One key event in the tumorigenic process is activation of survival signals, which can prevent cell death induced by DNA damage and/or oncogene activation (reviewed in Halazonetis et al., 2008). We used *S. cerevisiae* transformed with a CdtB-expressing plasmid as a model for intoxicated cells and screened a yeast deletion library to identify novel genes required for the CdtB-induced survival response (Fig. 1A and Table 1).

A genome-wide screen for the cellular responses to CdtB in *S. cerevisiae* has been previously described by Kitagawa et al. (Kitagawa et al., 2007). The focus of their study was to characterize the DNA damage repair mechanisms induced by CDTs, whereas we were interested to identify RhoA-dependent effectors that regulate cell survival in intoxicated cells. The significant overlap between the genes identified in this study and those reported by Kitagawa and co-workers or Bennett et al. (Bennett et al., 2001), who identified effectors that confer resistance to ionizing radiation, validates our screen and support the reliability of the data presented.

An expected result of the screen was the demonstration that proteins involved in DNA repair were important for cell survival in cells expressing CdtB. More surprising was the enrichment of genes encoding for proteins that regulate endocytosis, specifically those controlling sorting of ubiquitylated cargos at multivesicular bodies (Fig. 1B and Table 1).

The role of FEN1 in the activation of RhoA, phosphorylation of MAPK p38 and formation of actin stress fibers in response to DNA DSBs has not been reported previously. FEN1 is a multifunction nuclease that possesses endonuclease activity required for the maturation of the Okazaki fragments during DNA replication and long-patch DNA-base-excision repair (Liu et al., 2004). FEN1 also has a 5′-exonuclease activity (EXO) required for correct homologous DNA recombination and a gap-dependent endonuclease (GEN) activity, which cleaves the single-stranded DNA region of gapped DNA duplex or DNA forks that generate DNA DSBs (Parrish et al., 2003; Zheng et al., 2005). It has been shown that the EXO and GEN activities can be abrogated by a Glu-to-Asp mutation in position 60

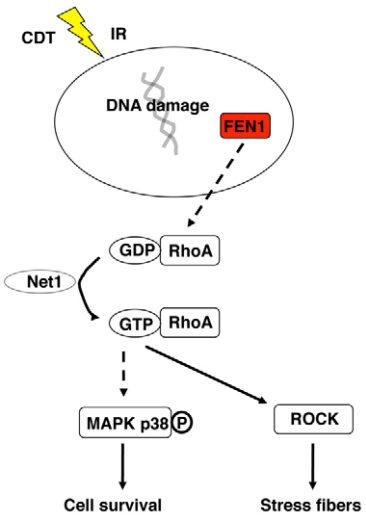

Fig. 6. Summary of the RhoA-dependent survival pathway. DNA damage leads to FEN1-dependent activation of RhoA, actin cytoskeleton remodeling, phosphorylation of MAPK p38 and prolonged cell survival.

(E60D), leading to frequent spontaneous mutations both in yeast and mammalian cells, and promotion of cancer progression in a knock-in mouse model (Zheng et al., 2007). These effects of FEN1 E60D are well in line with its role in maintenance of genomic stability. Interestingly, mouse embryo fibroblasts that expressing FEN1 E60D also show an increased susceptibility to cell death in response to UV irradiation compared with the cells that express wild-type FEN1, indicating that the EXO and/or GEN activities are required for cell survival in response to certain genotoxic stress. Our data demonstrate that the role of FEN1 in cell survival is also relevant in the response to DNA damage caused by the bacterial genotoxin CDT – and this is associated with activation of RhoA, formation of actin stress fibers and phosphorylation of MAPK p38 (Figs 3, 4 and 5). However, how FEN1 may induce activation of the small GTPase RhoA is presently not known.

We can envisage several possibilities. FEN1 is a protein that has been shown to regulate multiple pathways, such as genome integrity and fragmentation of apoptotic DNA (reviewed in Zheng et al., 2011). Its multitasking role is dependent on the sets of proteins that directly interact with FEN1, and can be further determined by its subcellular localization: nuclear and cytosolic (Qiu et al., 2001). To date 35 FEN1-interacting partners have been identified, which can be grouped into five functional categories: partners that regulate (i) DNA replication, (ii) DNA repair, (iii) DNA fragmentation during apoptosis, (iv) telomere stability and (v) post-translational modification of FEN1 (phosphorylation, acetylation and methylation) (reviewed in Zheng et al., 2011). In addition, a high throughput yeast two-hybrid screen has indicated that FEN1 directly interacts with the Rho GDP dissociation inhibitor (GDI) α (ARHGDIA) (Stelzl et al., 2005), suggesting that FEN1 performs additional activities not related to its endonuclease function. ARHGDIA maintains the small GTPase RhoA in an inactive form (DerMardirossian and Bokoch, 2005). It is conceivable that the fraction of FEN1 that is present in the cytosol sequesters ARHGDIA, allowing activation of RhoA upon of DNA damage. An independent DNA repair function has been previously demonstrated for other components of the DNA repair machinery. The DNA-dependent protein kinase DNA-PK, which forms a complex with the Ku heterodimer (Ku70–Ku80), is an essential component of the non-homologous end-joining recombination (NHEJ) (reviewed in Weterings and Chen, 2007). However, a fraction of DNA-PK is localized in the lipid raft microdomains of the plasma membrane (Lucero et al., 2003), and can phosphorylate Akt at Ser473 (Feng et al., 2004). Furthermore, the Ku70–Ku80 heterodimer has been shown to regulate cell adhesion to the extracellular matrix and to protect cells from apoptosis through suppression of the translocation of the pro-apoptotic protein Bax at the mitochondrial membrane (reviewed in Muller et al., 2005).

Another example of a membrane-associated protein that regulates NHEJ recombination is the cell polarity protein Par-3. This has long been considered to be a component of a complex that functions in the assembly of tight junctions, cell polarity and regulation of actin dynamics through interaction with the small GTPase Rac, which belongs to the Rho subfamily (Chen and Macara, 2005; Hurd and Margolis, 2005; Nishimura et al., 2005). Recently, Fang and colleagues have shown that Par-3 is also present in the nucleus and directly binds to the Ku heterodimer. This interaction is enhanced when cells are exposed to genotoxic stress (γ-irradiation or the anti-cancer agent etoposide phosphate), and knockdown of the protein by RNAi delays the DNA repair response and significantly decreases cell survival in response to ionizing radiation (Fang et al., 2007; Lees-Miller, 2007). These data demonstrate that there is an active crosstalk between the DNA repair machinery and proteins that are traditionally considered to be cytosolic and membrane related, such as Par-3 and small GTPases of the Rho family.

It is also possible that the FEN1-dependent activation of RhoA is a secondary effect of the DNA repair process. We have previously shown that DNA damage induced by ionizing radiation or CDT promotes dephosphorylation of the RhoA-specific GEF Net1 at the inhibitory site Ser152 (Alberts et al., 2005; Guerra et al., 2008b). Therefore, we cannot exclude that the FEN1-dependent DNA repair mechanisms, evoked by CDT or γ-irradiation, indirectly trigger Net1 dephosphorylation through the activation of a specific phosphatase or the inhibition of a kinase.

On the basis of the pathway enrichment analysis shown in Fig. 1B and the reported interaction with the RhoA effector ROCKI (Morita et al., 2007), we also tested the role of the ESCRT protein TSG101 in the regulation of RhoA activation and cell survival in HeLa cells exposed to CDT. Our results indicate that knockdown of TSG101 does not influence the rate of cell death and RhoA activation (Figs 3, 4 and 5). Our data suggest that the role of ESCRT proteins in cell survival upon induction of DNA damage is organism dependent. It is also possible that TSG101 regulates signaling that controls the extent of the cell cycle arrest upon induction of DNA damage rather than cell survival in *S. cerevisae* and, therefore, its deletion is associated with a prolonged arrest in G2 phase, which results in the marked delay in cell growth observed in the library screening (Fig. 1 and Table 1). Our data contribute to the understanding of poorly characterized aspects of cellular responses to genotoxic stress, such as the crosstalk between DNA repair and the cytosolic small GTPase RhoA (Fig. 6).

The identification of survival signals that are triggered by chronic infections of CDT-producing bacteria is crucial to understand whether these infections promote genomic instability and favor malignant transformation. The only bacterium classified as a human carcinogen is *Helicobacter pylori* (Crowe, 2005). However, a possible involvement in oncogenesis has been suggested for other bacteria, such as the Gram-negative bacterium *Salmonella typhi* (Lax, 2005). Establishing an association between infection with

Journal of Cell Science

Journal of Cell Science

CDT-producing bacteria and cancer promotion and/or progression might help the development of specific therapeutic protocols aimed at early and rapid eradication of the bacterial infection, thereby preventing an initial step of tumor development.

Materials and Methods

Cells

HeLa cells were obtained from ATCC and cultivated in RPMI 1640 medium supplemented with 10% fetal calf serum (FCS), 5 mM L-glutamine, penicillin (100 units/ml) and streptomycin (100 µg/ml) (complete medium) at 37°C in a humid atmosphere containing 5% CO_2.

Yeast strains and plasmids

The complete EUROpean *Saccharomyces cerevisiae* ARchive for Functional analysis (EUROSCARF) library, purchased from Open Biosystems, Thermo Scientific, consists of mutants where nonessential genes are individually deleted (Cherry et al., 1998). The pDCH-CdtB and the control plasmids have been previously described (Hassane et al., 2001).

The library and the control BY4743 strain (*MATa/MATα, his3Δ1/his3Δ1, leu2Δ/leu2Δmet15Δ0/MET15, LYS2/lys2Δ0, ura3Δ0/ura3Δ0*) were transformed with the pDCH-CdtB (Hassane et al., 2001) or a vector control plasmid. Dropout synthetic medium was prepared according to the manufacturer's instructions (Clontech). Transformants were selected and maintained in synthetic dropout medium without leucine (selective medium) supplemented with 2% glucose. For induction of CdtB expression, cells were grown in selective medium supplemented with 2% galactose and 2% raffinose.

Yeast transformation

Systematic yeast transformation experiments were performed, with minor modifications, using the *S. cerevisiae* direct transformation in a 96-well format, as previously described by (Schafer and Wolf, 2005). Yeast deletion strains were grown on yeast extract/peptone/glucose (YPGluc) square plates (12cm×12cm, Greiner Bio-one) for 48 hours at 30°C. Twenty-five microliters of the transformation solution (27% PEG600, 200 mM Lithium acetate, 50 mM DTT, carrier DNA 5 µg/µl, and 15 µg of the pDCH-CdtB or control plasmids) were added in 96-well plates and the yeast deletion strains were transferred using a 48-pin replicator, mixed well and incubated for 2 hours at 42°C. After mixing, 10 µl aliquots of the mixture were transferred on plates of synthetic dropout selective medium containing 2% glucose using a multi-channel pipette. Plates were let to dry at 22°C and incubated for 4 days at 30°C.

Confirmation PCR for the yeast deletion mutants

PCR was performed as previously described in the Single Tube Confirmation PCR Protocol (http://www-sequence.stanford.edu/group/yeast_deletion_project/single_tube_protocol.html). Briefly, one colony was suspended in 50 µl of 60U/ml zymolase 20T solution (Seikagaku Corporation) and incubated at 37°C for 1 hour, followed by 10 minutes at 95°C. PCR was performed as followed: 100 pmol of each primer was added in the PCR tubes containing 5 µl of yeast suspension. The PCR master mix was added and the PCR was carried out accordingly using the following conditions: Step1, 3 minutes at 95°C; Step 2, 15 seconds at 94°C, 15 seconds at 57°C, 1 minutes at 72°C, repeated for 35 cycles; Step3, 3 minutes at 72°C. PCR products were analyzed in 1.5% agarose gels.

Characterization of CdtB hypersensitive strains

To identify the CdtB hypersensitive mutants, transformants were picked, transferred to 100 µl of sterile H_2O in 96-well plates, and diluted to an optical density at 600 nm (OD_{600}) of 1. Five microliters of fivefold dilution series were transferred onto 10-cm diameter round plates containing selective medium supplemented with 2% glucose (CdtB OFF) or 2% galactose/raffinose (CdtB ON) using a 48-pin replicator and incubated at 30°C for 48 hours. Yeast strains that did not grow after the third dilution step in raffinose/galactose in three independent screens were considered as CdtB hypersensitive.

Flow cytometry analysis

Yeast cells were centrifuged at 3000 ***g*** for 5 minutes and the cell pellet was resuspended and fixed with 1 ml 70% ethanol at 4°C for at least 24 hours. After an additional centrifugation at 3000 ***g*** for 5 minutes, cells were resuspended in 0.8 ml RNase solution (50 mM Tris-HCl pH 7.8, 20 µg/ml RNase) and incubated overnight at 37°C. Samples were centrifuged and resuspended in 0.5 ml PI solution (200 mM Tris-HCl pH 7.5, 211 mM NaCl, 78 mM $MgCl_2$, 25 µg/ml propidium iodide), and sonicated for 5 seconds at medium voltage. Thirty microliters of cell suspension was mixed in a tube together with 0.6 ml 50 mM Tris-HCl pH 7.5. Samples were analyzed with a FACS Calibure flow cytometer. Data from ~30,000 cells were collected and analyzed using the CellQuest software.

Bioinformatic analysis

The 59 human orthologs of yeast genes were identified using the Inparanoid database (O'Brien et al., 2005), BLAST sequence alignment against all human protein sequences and literature search. These genes were used as input into the DAVID bioinformatic resource available at http://david.abcc.ncifcrf.gov (Dennis et al., 2003). Pathway enrichment analysis was conducted using the functional annotation clustering tool for testing the over-representation of genes in particular pathways from the Kyoto Encyclopedia of Genes and Genomes (KEGG) pathway database (Kanehisa et al., 2010).

This test uses a standard Fisher exact test. A Bonferroni multiple testing and a *P*-value (Ease score) of 0.1 and fold enrichment of at least 1.5 were applied as standard cut-off level.

Identification of the proteins interacting with the RhoA signaling pathway

The RhoA protein–protein interaction network was generated using the protein interaction network analysis (PINA) (Wu et al., 2009) integrated platform. PINA integrates protein–protein interaction data from six curated databases (MINT, IntAct, BioGRID, HPRD amd MIPS/MPact) including experimentally validated and computationally predicted interaction data (only experimentally reported interactions were used for our analysis). We then examined whether any of the proteins encoded by the human orthologs present in our data set share common interacting partners with RhoA.

CDT and treatments

Production of the *H. ducreyi* CdtB was as previously described (Frisan et al., 2003). His-tagged CdtA and CdtC were constructed by PCR amplification of the *H. ducreyi cdtA* and *cdtC* genes from the pAF-tac1cdtA and pAF-tac1cdtC plasmids, respectively (Frisk et al., 2001) using the following primers: CdtA_F 5′-ATTCGGATCCATGTTCATCAAATCAACGAATGA-3′, CdtA_R 5′-TACCGAATTCTTAATTAACCGCTGTTGCTTCTAAT-3′, CdtC_F 5′- ATTCGGATCCAAGTCATGCAGAATCAAATCCTGA-3, CdtC_R 5′-5′-TACCGAATTCTTAGCTACCCTGATTTCTT-3′. Each PCR fragment was cloned into the *Bam*HI and *Eco*RI restriction sites of the pACYC-Duet-1 expression vector (Novagen). Purification of the His-tagged CdtA and CdtC subunits from inclusion bodies was performed as previously described (Moberg et al., 2004). Reconstitution of the active holotoxin (named as CDT) was as previously described (Frisan et al., 2003).

Toxin treatment

Cells were incubated for the indicated time periods with CDT (2 µg/ml) in complete medium.

Ionizing radiation

Cells were irradiated (20 Gy), washed once with PBS and incubated for indicated time periods in complete medium.

RNA interference and transfections

A total of 10^5 HeLa cells were plated in 12-well plates in 1 ml of medium. Transfection was performed using the forward protocol with the INTERFERin™ reagent (Polyplus Transfection™), according to the manufacturer's instructions. Gene silencing was assessed by western blot analysis 48 hours after transfection. The following duplex small interfering RNAs (siRNAs) were used: Hs_FEN1_6 #SI02663451 (FEN1_1); Hs_TSG101_6 #SI02655184 (TSG101_1); Hs_TSG101_7 #SI02664522 (TSG101_2); Hs_CSNK2B_5 #SI00605185 (CSNK2B _1); Hs_CSNK2B_6 #SI00605192 (CSNK2B _1); Allstars Negative Control siRNA #102780 (scRNA), all from Qiagen; and FEN1 s5103 (FEN1_2) from Applied Biosystems, Ambion.

Immunofluorescence

Immunofluorescence analysis was performed as previously described (Frisan et al., 2003; Guerra et al., 2008a), using the conformation-dependent monoclonal antibody (6A7, BD Pharmingen), which recognizes the active form of Bax. The actin cytoskeleton was visualized by staining with TRITC-phalloidin, as previously described (Frisan et al., 2003). Nuclei were counterstained with DAPI (Vector Laboratories Inc). Slides were mounted and viewed using a Leica DMRXA fluorescence microscope with a CCD camera (Hammamatsu), and images were captured using Improvision Openlab v.2 software. The TRITC-phalloidin fluorescence intensity and the cell area were measured using ImageJ software (http://rsbweb.nih.gov/ij/).

RhoA activation

RhoA activation was assessed using the G-LISA™ RhoA Activation Assay Biochem Kit™ (Cytoskeleton), according to the instructions of the manufacturer.

Western blot analysis

Proteins were fractionated by SDS-polyacrylamide gels, transferred to PVDF membranes (Millipore) and probed with the antibodies against phosphorylated MAPK p38, MAPK p38, FEN1 (Cell Signaling), TSG101 and actin (Sigma). Blots were developed with enhanced chemoluminescence, using the appropriate horseradish peroxidase-labelled secondary antibody, according to the instructions of the manufacturer (GE Healthcare).

Journal of Cell Science

Statistical analysis

To evaluate the significance of the results, the independent two-sample *t*-test was performed using the SPSS® software from IBM. Plotting histograms and box-whisker graph was used to check the assumption of Normality of continuous data.

This work has been supported by the Swedish Research Council, the Swedish Cancer Society, the Åke-Wiberg Foundation, the Magnus Bergvall Fundation and the Karolinska Institutet to T.F., the Robert Lundberg Memorial Fundation to L.G., the European Community Integrated Project on Infection and Cancer (INCA), Project no. LSHC-CT-2005-018704 to M.G.M. The Swedish Cancer Society supports T.F.

Supplementary material available online at
http://jcs.biologists.org/cgi/content/full/124/16/2735/DC1

References

Alberts, A. S., Qin, H., Carr, H. S. and Frost, J. A. (2005). PAK1 negatively regulates the activity of the Rho exchange factor NET1. *J. Biol. Chem.* **280**, 12152-12161.

Bennett, C. B., Lewis, L. K., Karthikeyan, G., Lobachev, K. S., Jin, Y. H., Sterling, J. F., Snipe, J. R. and Resnick, M. A. (2001). Genes required for ionizing radiation resistance in yeast. *Nat. Genet.* **29**, 426-434.

Chen, X. and Macara, I. G. (2005). Par-3 controls tight junction assembly through the Rac exchange factor Tiam1. *Nat. Cell Biol.* **7**, 262-269.

Cherry, J. M., Adler, C., Ball, C., Chervitz, S. A., Dwight, S. S., Hester, E. T., Jia, Y., Juvik, G., Roe, T., Schroeder, M. et al. (1998). SGD: Saccharomyces Genome Database. *Nucleic Acids Res.* **26**, 73-79.

Cortes-Bratti, X., Chaves-Olarte, E., Lagergård, T. and Thelestam, M. (1999). The cytolethal distending toxin from the chancroid bacterium *Haemophilus ducreyi* induces cell-cycle arrest in the G2 phase. *J. Clin. Invest.* **103**, 107-115.

Cortes-Bratti, X., Karlsson, C., Lagergard, T., Thelestam, M. and Frisan, T. (2001). The *Haemophilus ducreyi* cytolethal distending toxin induces cell cycle arrest and apoptosis via the DNA damage checkpoint pathways. *J. Biol. Chem.* **276**, 5296-5302.

Crowe, S. E. (2005). Helicobacter infection, chronic inflammation, and the development of malignancy. *Curr. Opin. Gastroenterol.* **21**, 32-38.

Dennis, G., Jr, Sherman, B. T., Hosack, D. A., Yang, J., Gao, W., Lane, H. C. and Lempicki, R. A. (2003). DAVID: Database for Annotation, Visualization, and Integrated Discovery. *Genome Biol.* **4**, P3.

DerMardirossian, C. and Bokoch, G. M. (2005). GDIs: central regulatory molecules in Rho GTPase activation. *Trends Cell Biol.* **15**, 356-363.

Elwell, C., Chao, K., Patel, K. and Dreyfus, L. (2001). *Escherichia coli* CdtB mediates cytolethal distending toxin cell cycle arrest. *Infect. Immun.* **69**, 3418-3422.

Fang, L., Wang, Y., Du, D., Yang, G., Tak Kwok, T., Kai Kong, S., Chen, B., Chen, D. J. and Chen, Z. (2007). Cell polarity protein Par3 complexes with DNA-PK via Ku70 and regulates DNA double-strand break repair. *Cell Res.* **17**, 100-116.

Feng, J., Park, J., Cron, P., Hess, D. and Hemmings, B. A. (2004). Identification of a PKB/Akt hydrophobic motif Ser-473 kinase as DNA-dependent protein kinase. *J. Biol. Chem.* **279**, 41189-41196.

Frisan, T., Cortes-Bratti, X., Chaves-Olarte, E., Stenerlöw, B. and Thelestam, M. (2003). The *Haemophilus ducreyi* cytolethal distending toxin induces DNA double strand breaks and promotes ATM-dependent activation of RhoA. *Cell. Microbiol.* **5**, 695-707.

Frisk, A., Lebens, M., Johansson, C., Ahmed, H., Svensson, L., Ahlman, K. and Lagergård, T. (2001). The role of different protein components from the *Haemophilus ducreyi* cytolethal distending toxin in the generation of cell toxicity. *Microb. Pathog.* **30**, 313-324.

Gelfanova, V., Hansen, E. J. and Spinola, S. M. (1999). Cytolethal distending toxin of *Haemophilus ducreyi* induces apoptotic death of Jurkat T cells. *Infect. Immun.* **67**, 6394-6402.

Guerra, L., Carr, H. S., Richter-Dahlfors, A., Masucci, M. G., Thelestam, M., Frost, J. A. and Frisan, T. (2008a). A bacterial cytotoxin identifies the RhoA exchange factor Net1 as a key effector in the response to DNA damage. *PLoS ONE* **3**, e2254.

Guerra, L., Nemec, K. N., Massey, S., Tatulian, S. A., Thelestam, M., Frisan, T. and Teter, K. (2008b). A novel mode of translocation for cytolethal distending toxin. *Biochim. Biophys. Acta* **1793**, 489-495.

Halazonetis, T. D., Gorgoulis, V. G. and Bartek, J. (2008). An oncogene-induced DNA damage model for cancer development. *Science* **319**, 1352-1355.

Hassane, D. C., Lee, R. B., Mendenhall, M. D. and Pickett, C. L. (2001). Cytolethal distending toxin demonstrates genotoxic activity in a yeast model. *Infect. Immun.* **69**, 5752-5759.

Hassane, D. C., Lee, R. B. and Pickett, C. L. (2003). *Campylobacter jejuni* cytolethal distending toxin promotes DNA repair responses in normal human cells. *Infect. Immun.* **71**, 541-545.

Hurd, T. W. and Margolis, B. (2005). Pars and polarity: taking control of Rac. *Nat. Cell Biol.* **7**, 205-207.

Kanehisa, M., Goto, S., Furumichi, M., Tanabe, M. and Hirakawa, M. (2010). KEGG for representation and analysis of molecular networks involving diseases and drugs. *Nucleic Acids Res.* **38**, D355-D360.

Kastan, M. B. and Bartek, J. (2004). Cell-cycle checkpoints and cancer. *Nature* **432**, 316-323.

Kitagawa, T., Hoshida, H. and Akada, R. (2007). Genome-wide analysis of cellular response to bacterial genotoxin CdtB in yeast. *Infect. Immun.* **75**, 1393-1402.

Lara-Tejero, M. and Galan, J. E. (2000). A bacterial toxin that controls cell cycle progression as a deoxyribonuclease I-like protein. *Science* **290**, 354-357.

Lara-Tejero, M. and Galan, J. E. (2001). CdtA, CdtB and CdtC form a tripartite complex that is required for cytolethal distending toxin activity. *Infect. Immun.* **69**, 4358-4365.

Lax, A. J. (2005). Bacterial toxins and cancer – a case to answer? *Nat. Rev. Microbiol.* **3**, 343-349.

Lee, R. B., Hassane, D. C., Cottle, D. L. and Pickett, C. L. (2003). Interactions of *Campylobacter jejuni* cytolethal distending toxin subunits CdtA and CdtC with HeLa cells. *Infect. Immun.* **71**, 4883-4890.

Lees-Miller, S. P. (2007). The double (strand break) life of Par-3. *Nat. Cell Biol.* **9**, 363-365.

Li, L., Sharipo, A., Chaves-Olarte, E., Masucci, M. G., Levitsky, V., Thelestam, M. and Frisan, T. (2002). The *Haemophilus ducreyi* cytolethal distending toxin activates sensors of DNA damage and repair complexes in proliferating and non-proliferating cells. *Cell. Microbiol.* **4**, 87-99.

Liu, Y., Kao, H. I. and Bambara, R. A. (2004). Flap endonuclease 1, a central component of DNA metabolism. *Annu. Rev. Biochem.* **73**, 589-615.

Lucero, H., Gae, D. and Taccioli, G. E. (2003). Novel localization of the DNA-PK complex in lipid rafts: a putative role in the signal transduction pathway of the ionizing radiation response. *J. Biol. Chem.* **278**, 22136-22143.

McSweeney, L. A. and Dreyfus, L. A. (2004). Nuclear localization of the *Escherichia coli* cytolethal distending toxin CdtB subunit. *Cell. Microbiol.* **6**, 447-458.

McSweeney, L. A. and Dreyfus, L. A. (2005). Carbohydrate-binding specificity of the *Escherichia coli* cytolethal distending toxin CdtA-II and CdtC-II subunits. *Infect. Immun.* **73**, 2051-2060.

Moberg, P., Nilsson, S., Stahl, A., Eriksson, A. C., Glaser, E. and Maler, L. (2004). NMR solution structure of the mitochondrial F1beta presequence from *Nicotiana plumbaginifolia*. *J. Mol. Biol.* **336**, 1129-1140.

Morita, E., Sandrin, V., Chung, H. Y., Morham, S. G., Gygi, S. P., Rodesch, C. K. and Sundquist, W. I. (2007). Human ESCRT and ALIX proteins interact with proteins of the midbody and function in cytokinesis. *EMBO J.* **26**, 4215-4227.

Muller, C., Paupert, J., Monferran, S. and Salles, B. (2005). The double life of the Ku protein: facing the DNA breaks and the extracellular environment. *Cell Cycle* **4**, 438-441.

Nesic, D., Hsu, Y. and Stebbins, C. E. (2004). Assembly and function of a bacterial genotoxin. *Nature* **429**, 429-433.

Nishimura, T., Yamaguchi, T., Kato, K., Yoshizawa, M., Nabeshima, Y., Ohno, S., Hoshino, M. and Kaibuchi, K. (2005). PAR-6-PAR-3 mediates Cdc42-induced Rac activation through the Rac GEFs STEF/Tiam1. *Nat. Cell Biol.* **7**, 270-277.

O'Brien, K. P., Remm, M. and Sonnhammer, E. L. (2005). Inparanoid: a comprehensive database of eukaryotic orthologs. *Nucleic Acids Res.* **33**, D476-D480.

Parrish, J. Z., Yang, C., Shen, B. and Xue, D. (2003). CRN-1, a *Caenorhabditis elegans* FEN-1 homologue, cooperates with CPS-6/EndoG to promote apoptotic DNA degradation. *EMBO J.* **22**, 3451-3460.

Qiu, J., Li, X., Frank, G. and Shen, B. (2001). Cell cycle-dependent and DNA damage-inducible nuclear localization of FEN-1 nuclease is consistent with its dual functions in DNA replication and repair. *J. Biol. Chem.* **276**, 4901-4908.

Schafer, A. and Wolf, D. H. (2005). Endoplasmic reticulum-associated protein quality control and degradation: screen for ERAD mutants after ethylmethane sulfonate mutagenesis. *Methods Mol. Biol.* **301**, 283-288.

Scott, D. A. and Kaper, J. B. (1994). Cloning and sequencing of the genes encoding *Escherichia coli* cytolethal distending toxins. *Infect. Immun.* **62**, 244-251.

Shiloh, Y. (2003). ATM and related protein kinases: safeguarding genome integrity. *Nat. Rev. Cancer* **3**, 155-168.

Smith, J. L. and Bayles, D. O. (2006). The contribution of cytolethal distending toxin to bacterial pathogenesis. *Crit. Rev. Microbiol.* **32**, 227-248.

Stelzl, U., Worm, U., Lalowski, M., Haenig, C., Brembeck, F. H., Goehler, H., Stroedicke, M., Zenkner, M., Schoenherr, A., Koeppen, S. et al. (2005). A human protein-protein interaction network: a resource for annotating the proteome. *Cell* **122**, 957-968.

Weterings, E. and Chen, D. J. (2007). DNA-dependent protein kinase in nonhomologous end joining: a lock with multiple keys? *J. Cell Biol.* **179**, 183-186.

Wu, J., Vallenius, T., Ovaska, K., Westermarck, J., Makela, T. P. and Hautaniemi, S. (2009). Integrated network analysis platform for protein-protein interactions. *Nat. Methods* **6**, 75-77.

Zheng, L., Zhou, M., Chai, Q., Parrish, J., Xue, D., Patrick, S. M., Turchi, J. J., Yannone, S. M., Chen, D. and Shen, B. (2005). Novel function of the flap endonuclease 1 complex in processing stalled DNA replication forks. *EMBO Rep.* **6**, 83-89.

Zheng, L., Dai, H., Zhou, M., Li, M., Singh, P., Qiu, J., Tsark, W., Huang, Q., Kernstine, K., Zhang, X. et al. (2007). Fen1 mutations result in autoimmunity, chronic inflammation and cancers. *Nat. Med.* **13**, 812-819.

Zheng, L., Jia, J., David Finger, L., Guo, Z., Zer, C. and Shen, B. (2011). Functional regulation of FEN1 nuclease and its link to cancer. *Nucleic Acids Res.* **29**, 781-794.